

The Role of Typhoon Songda (2004) in Producing Distantly Located Heavy Rainfall in Japan*

YONGQING WANG

Pacific Typhoon Research Center, KLME, Nanjing University of Information Science and Technology, Nanjing, China, and International Pacific Research Center and Department of Meteorology, University of Hawaii at Manoa, Honolulu, Hawaii

YUQING WANG

International Pacific Research Center and Department of Meteorology, University of Hawaii at Manoa, Honolulu, Hawaii, and Pacific Typhoon Research Center, KLME, Nanjing University of Information Science and Technology, Nanjing, China

HIRONORI FUDEYASU

International Pacific Research Center and Department of Meteorology, University of Hawaii at Manoa, Honolulu, Hawaii

(Manuscript received 5 January 2009, in final form 20 May 2009)

ABSTRACT

When Typhoon Songda (2004) was located southeast of Okinawa over the western North Pacific during 2–4 September 2004, a heavy rainfall event occurred over southern central Japan and its adjacent seas, more than 1200 km from the typhoon center. The Advanced Research version of the Weather Research and Forecast (WRF-ARW) model was used to investigate the possible remote effects of Typhoon Songda on this heavy precipitation event in Japan. The National Centers for Environmental Prediction (NCEP) global final (FNL) analysis was used to provide both the initial and lateral boundary conditions for the WRF model. The model was initialized at 1800 UTC 2 September and integrated until 1800 UTC 6 September 2004, during which Songda was a supertyphoon. Two primary numerical experiments were performed. In the control experiment, a bogus vortex was inserted into the FNL analysis to enhance the initial storm intensity such that the model typhoon had an intensity that was similar to that observed at the initial time. In the no-typhoon experiment, the vortex associated with Typhoon Songda in the FNL analysis was removed by a smoothing algorithm such that the typhoon signal did not appear at the initial time. As verified against various observations, the control experiment captured reasonably well the evolution of the storm and the spatial distribution and evolution of the precipitation, whereas the remote precipitation in Japan was largely suppressed in the no-typhoon experiment, indicating the significant far-reaching effects of Typhoon Songda. Songda enhanced the remote precipitation in Japan mainly through northward moisture transport into the preconditioned precipitation region by its outer circulation. The orographic forcing of the central mountains in Japan played a small role compared with Typhoon Songda in this extreme precipitation event.

* School of Ocean and Earth Science and Technology Publication Number 7802 and International Pacific Research Center Publication Number 630.

Corresponding author address: Dr. Yuqing Wang, IPRC/SOEST, University of Hawaii at Manoa, Post Bldg. 409G, 1680 East-West Rd., Honolulu, HI 96822.
E-mail: yuqing@hawaii.edu

1. Introduction

Tropical cyclones (TCs, or typhoons in the western North Pacific, hurricanes in the Atlantic or eastern North Pacific) are often heavy rain producers. In particular, landfalling TCs usually cause fatalities and economic losses due to not only strong winds but also torrential rainfall that often induces flash flooding after their landfall (e.g., Kunkel et al. 1999). A TC can produce

tremendous rainfall in its eyewall and as well as in both its inner and outer spiral rainbands, which may be several tens to hundred kilometers from the TC center (Takahashi and Kawano 1998; Lonfat et al. 2007; Kimball 2008; Yokoyama and Takayabu 2008). This is generally referred to as direct effect of a TC on precipitation, or precipitation induced by the TC itself. On the other hand, when a strong interaction with other synoptic systems occurs, a TC can induce heavy rainfall far away, for example, beyond a thousand kilometers from its center. Such an effect of a TC on precipitation in a remote area is generally referred to as indirect or remote effect of a TC on precipitation (Bosart and Carr 1978; Ross and Kurihara 1995; Chen et al. 2006).

Although most TCs mainly produce heavy rainfall directly by themselves (direct effect), some TCs can induce heavy rainfall in remote areas when they interact with other synoptic systems, such as upper-level trough and cold frontal systems in the midlatitudes (indirect effect). This latter effect, which does not occur very often, usually causes an even greater disaster when it does happen because special attention is mostly given to precipitation directly caused by the TC itself (Chen et al. 2006). Quantitative precipitation forecasts (QPF) are very important whereas they are quite challenging to operational forecasters. Current skill in QPF, including the forecast of TC precipitation (Elsberry 2002), is quite low. In particular, the forecast skill for TC precipitation is largely affected by the prediction accuracy of the TC track (Chen et al. 2006; Marchok et al. 2007).

Previous studies have mostly focused on precipitation directly caused by a TC either over the open ocean (e.g., Wang and Holland 1996a,b; Rogers et al. 2003; Atallah et al. 2007) or approaching–making landfall (e.g., Li et al. 2007; Kimball 2008; Chen et al. 2006). These studies have shown that over the open ocean, the rainfall distribution in a TC is largely controlled by the vertical shear in the large-scale environmental flow and the translation speed of the storm itself; however, after landfall, both the rainfall intensity and the radial extent of the outer rainfall are also affected by the soil moisture of the underlying land surface.

Some studies have also investigated the indirect effects of a TC on remote precipitation. Bosart and Carr (1978) were among the first to document a case study for an excessive rainfall event due to the indirect effects of Hurricane Agnes (1972). They showed that a weak short wave in the mid- to upper troposphere provided the initial triggering mechanism for the growth of the rain area while Agnes's circulation transported plentiful moisture from the western Atlantic to the rain area, enhancing the rainfall greatly. Murata (Chen et al. 2006) studied the Typhoon Meari (2004) case. Typhoon Meari made landfall

in Kyushu in Japan and resulted in heavy rainfall along the Kii Peninsula, more than 500 km to the east of the typhoon center. He performed a series of sensitivity numerical experiments and demonstrated that the moisture supplied by the typhoon's outer circulation and the interaction with topography played critical roles in the heavy rainfall. Farfán and Fogel (2007) investigated the influence of eastern Pacific TC circulations on the distribution of humidity and convection over northwest Mexico. They suggested that TC activities serve as a source of humid tropical air masses, providing conditions that support deep convection and that, thus, cause heavy rainfall over northwest Mexico. Another category of the indirect effect is the downstream impacts of TCs that experience extratropical transition. As was recently demonstrated by Harr et al. (2008), a recurving TC undergoing extratropical transition over the northwest Pacific could perturb the upper-level westerly jet stream in the midlatitude, exciting Rossby waves in the westerlies and impacting the midlatitude circulation and weather far downstream over the North America.

One more category of the indirect effect of a TC on remote precipitation is the remote heavy rainfall resulting from the interaction between a TC over the open ocean and a weather system (such as a cold frontal system) far away from the TC center. This type of remote effect from a typhoon over the northwest Pacific on the circulation and precipitation in Japan was previously studied by Kawamura and Ogasawara (2006) and Yamada and Kawamura (2007) with the use of reanalysis data. They found that one or two typhoons, which might serve as synoptic convective heating sources over the northwest Pacific, could induce the quasi-stationary barotropic Rossby wave train emanating northeastward and significantly affect the anomalous weather in the vicinity of Japan. This teleconnection was called the Pacific–Japan (PJ) pattern. They suggested that the establishment of the PJ pattern intensifies the east–west pressure gradient at low levels between a typhoon and an anomalous anticyclone east of Japan, which enhances the warm advection and moisture supply from low latitudes to the vicinity of Japan, thus causing remote precipitation in Japan.

A case study for a similar scenario including the indirect effects of a typhoon on remote precipitation in Japan is investigated numerically here. The case chosen in our study was Typhoon Songda (2004), which caused heavy rainfall in southern central Japan and its adjacent seas when it was far away from the heavy precipitation region. The Advanced Research version of the Weather Research and Forecasting (WRF) model developed at the National Center for Atmospheric Research (NCAR) is used to perform two major simulations, one with and one without the typhoon circulation, to highlight the

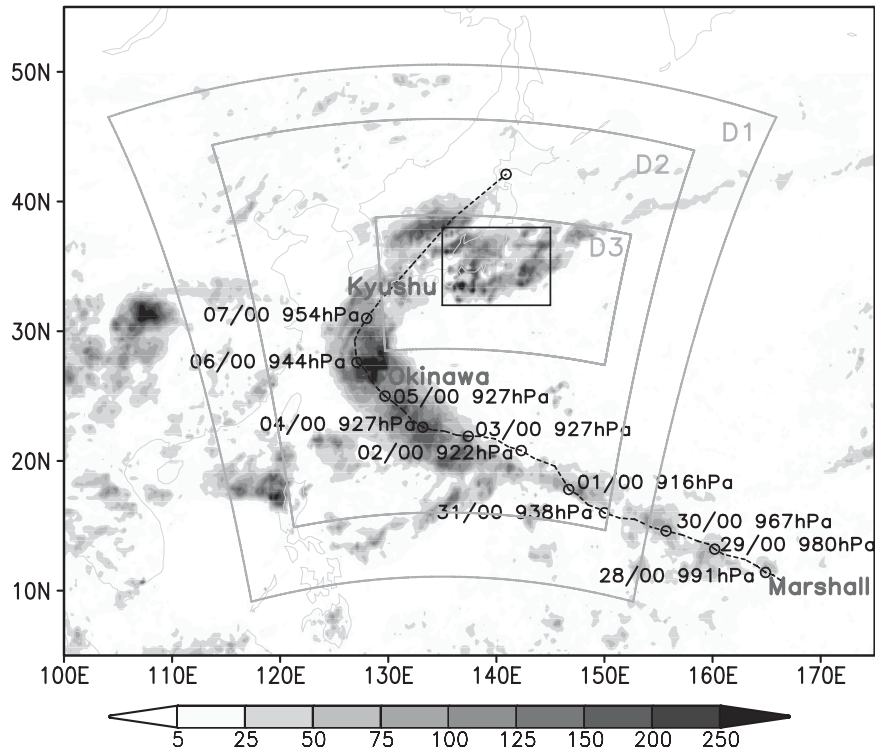


FIG. 1. Total precipitation (mm) between 1800 UTC 2 Sep and 0000 UTC 5 Sep 2004 and the best track of Typhoon Songda (2004) from JTWC (information online at <http://metocph.nmci.navy.mil/jtwc>). The TRMM 3B42 V6 3-hourly merged rainfall dataset, which was obtained from the Asia-Pacific Data Research Center (APDRC) at the University of Hawaii, was used. The same precipitation dataset was used as the observed precipitation in Fig. 10 as well. The small box in D3 shows the area of interest that will be used for area averaging in Fig. 10.

effects of Typhoon Songda (2004) on remote precipitation and to investigate the involved physical mechanisms. Several supplementary experiments are performed to examine the potential effects of topography over Japan and the radial wind profile of the typhoon itself on the simulated remote precipitation.

The rest of the paper is organized as follows. The next section provides a brief overview of Typhoon Songda (2004) and its possible contributions to the heavy rainfall in Japan. Section 3 describes the basic features of the WRF model and the experimental design, including methodologies to enhance the initial typhoon vortex or remove the typhoon from the initial conditions. Results from the control simulation are verified with various available datasets in section 4. The effects of Typhoon Songda on remote precipitation in Japan and the physical mechanisms involved are discussed in section 5. Major findings are summarized in section 6.

2. An overview of Typhoon Songda

Typhoon Songda (2004) was 1 of the 10 named typhoons that made landfall on the main islands of Japan

in 2004 and brought extensive damage to Japan due to both strong winds and heavy rainfall (Nakazawa and Rajendran 2007). The storm formed near the Marshall Islands on 27 August 2004 and moved northwestward over the western North Pacific. After passing the Okinawa Islands, it recurved northeastward over the East China Sea on 1200 UTC 6 September and then made landfall on Kyushu Island, south of the main island of Japan, at 0000 UTC 7 September (Fig. 1). Songda reached its lifetime peak intensity with a maximum sustained near-surface wind speed of 64 m s^{-1} and a minimum central sea level pressure of 916 hPa.

Similar to many other typhoons, Songda produced heavy rainfall along its track under its eyewall and in its major spiral rainbands (Fig. 1). When Typhoon Songda was located more than 1500 km south of the main islands of Japan over the western North Pacific during 1800 UTC 2 September–0000 UTC 5 September, a rainband with several strong convective cores occurred over the southern central Japan and the adjacent sea (32° – 38° N, 135° – 145° E; see the black box in Fig. 1). It is our hypothesis that in addition to the heavy rainfall directly associated with deep convection in the inner core, Typhoon Songda

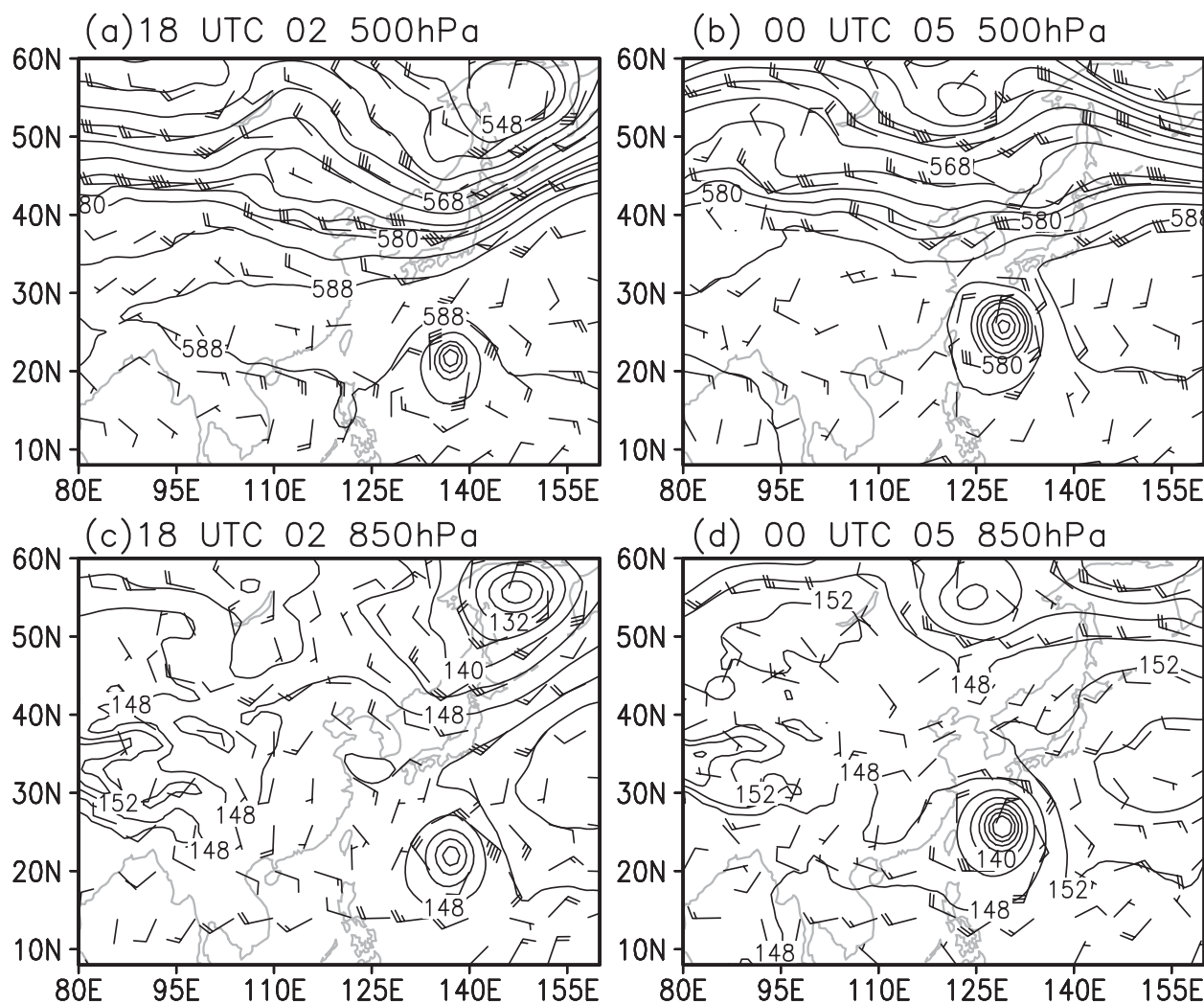


FIG. 2. The geopotential height (10 gpm contours) and wind field (barbs) at (top) 500 and (bottom) 850 hPa with a contour interval of 40 gpm from the FNL analysis for (left) 1800 UTC 2 Sep and (right) 0000 UTC 5 Sep 2004. One flag represents 50 kt and one full barb represents 10 kt.

contributed significantly to the heavy rainfall over southern central Japan and the adjacent sea because its outer circulation to the east transported moisture northward to the preconditioned local precipitation system. This can be considered to be the indirect effect of Typhoon Songda on precipitation in a remote area as discussed in section 1. Although the topography in the central Japan might play a role in enhancing the heavy precipitation in Japan, the numerical results in section 5 demonstrate that the orographic effect is insignificant in the Songda case.

Figure 2 shows the synoptic patterns at 1800 UTC 2 September and 0000 UTC 5 September 2004 at 500 and 850 hPa. Typhoon Songda was located south of the east-west-elongated subtropical ridge and embedded in the southeasterly flow on the southwestern edge of the western Pacific subtropical anticyclone at 1800 UTC 2 Sep-

tember (Figs. 2a and 2c). To the north in the midlatitudes was a short-wave trough embedded in the westerly jet stream at 500 hPa over the Japan Sea. In addition to the main subtropical anticyclone to the east around 30°N, there were subtropical anticyclonic cells at both 500 and 850 hPa over southeastern China (Figs. 2a and 2c). This gave rise to a northeast-southwest-elongated region with considerable cyclonic shear and low-level convergence between the two anticyclonic circulations over the main islands of Japan. This situation favored the upward motion and moisture convergence and served as a triggering mechanism for precipitation in the region in the coming 2–3 days (see further discussion below). By 0000 UTC 5 September, the short-wave trough in the westerlies moved eastward out of the domain and the jet stream in the midlatitude weakened considerably with the development

of a short-wave trough and ridge pair farther to the north of the Japan Sea at 500 hPa (Fig. 2b). In the lower troposphere, the cyclonic shear with horizontal wind convergence was still over Japan but it had weakened considerably, and now Typhoon Songda was approaching the main islands of Japan from the southwest (Fig. 2d).

Accompanied by the large-scale circulation given in Fig. 2 was a northeast–southwest-elongated region with cyclonic shear at the surface off the southeast coast of the main islands of Japan (Fig. 3a) and a short-wave trough farther to the north over the Japan Sea. The short-wave trough moved eastward in the following 12 h and arrived at the eastern coast of northern Japan, and the cyclonic shear line moved to the southeast (Fig. 3b). In the next 12 h, the short-wave trough moved eastward slowly, whereas the cyclonic shear line shifted northwestward toward southern Japan and aligned itself with the short-wave trough to the north by 1800 UTC 3 September (Fig. 3c). Corresponding to the surface wind fields was a northeast–southwest-elongated cyclonic vorticity zone in the lower troposphere over southern central Japan at 1800 UTC 2 September (Fig. 3d) with the development of low-level convergence by 0600 UTC 3 September (Fig. 3e). By 1800 UTC 3 September, a strong convergence zone at 850 hPa with upward motion (not shown) developed over southern central Japan and the adjacent seas. This is the time when significant rainfall started in the region. Therefore, the low-level cyclonic shear zone with strong horizontal wind convergence was the key to the vertical motion and thus was the preconditioning and initiation of precipitation over southern central Japan and the adjacent seas, where the troposphere was already conditionally unstable to cumulus convection (not shown). We will show in section 5 that the northward moisture transport by the low-level southerly–southeasterly flow of Songda's outer circulation was crucial to the subsequent heavy rainfall over Japan.

Figure 4 shows the satellite images over East Asia and the western North Pacific. There were two major cloud systems in the region: one to the southeast of the Okinawa Islands associated with Typhoon Songda and the other associated with the surface shear line across the main islands of Japan during 1200 UTC 3 September and 0600 UTC 4 September. Although interactions might exist between the two cloud systems, they were definitely separate systems during this period. After 0000 UTC 5 September, Typhoon Songda headed northeastward, approaching the main islands of Japan, and followed by the direct effects of the typhoon itself on precipitation in Japan. Since the focus of this study is on the indirect effects of Typhoon Songda on precipitation in Japan, our attention would thus be given to the period during 1800 UTC 2 September–0000 UTC 5 September 2004.

3. Model configuration and experimental design

a. Model configuration

The model used in this study is version 2.2.1 of the Advanced Research WRF (ARW) model developed at NCAR (Skamarock et al. 2008). WRF-ARW is a three-dimensional, fully compressible, nonhydrostatic model formulated within a terrain-following mass coordinate in the vertical. The model physics include the grid-scale cloud and precipitation scheme used in the new Eta Model, namely, the Ferrier cloud microphysics scheme (Ferrier 1994), the Rapid Radiative Transfer Model (RRTM) for longwave radiation (Mlawer et al. 1997), the Goddard shortwave radiation scheme (Chou and Suarez 1994), the Monin–Obukhov surface flux calculation over the ocean, the Rapid Update Cycle (RUC) land surface model (Smirnova et al. 1997, 2000), the Yonsei University (YSU) planetary boundary layer scheme (Hong et al. 2006), and the Kain–Fritsch cumulus parameterization scheme (Kain and Fritsch 1990) for subgrid-scale deep convection.

Three interactive nesting domains (Fig. 1) are used in all of the numerical experiments performed in this study. The outermost domain (D1) had 166×166 grid points, centered at 30°N , 135°E , with horizontal grid spacing of 27 km. The second domain (D2) had 370×370 grid points with horizontal grid spacing of 9 km. The innermost domain (D3) had 673×379 grid points with horizontal grid spacing of 3 km, which covers the precipitation region in Japan and the adjacent seas. The second domain (D2) was used to explicitly resolve the structure of the typhoon and the mesoscale precipitation systems, as was briefly discussed in section 2 above. The innermost domain (D3) was used to better resolve the fine structure of the frontal system near Japan. Note that the cumulus parameterization was not activated in D3. The model was run with 28 unevenly distributed vertical levels with higher resolution in the planetary boundary layer and with the model top at 10 hPa. The NCAR-archived National Centers for Environmental Prediction (NCEP) global final (FNL) analysis dataset at $1^\circ \times 1^\circ$ latitude–longitude grids and 6-h intervals was used to provide both the initial and lateral boundary conditions to the WRF-ARW model. Sea surface temperature (SST) used in the model simulation was taken from the NCEP real-time objective SST analysis with $0.5^\circ \times 0.5^\circ$ horizontal grid spacing at the initial time and did not change during the model simulation. This could be a limitation for the realistic simulation of the typhoon intensity.

b. Experimental design

Four numerical experiments were performed using the model configuration above in this study. The control

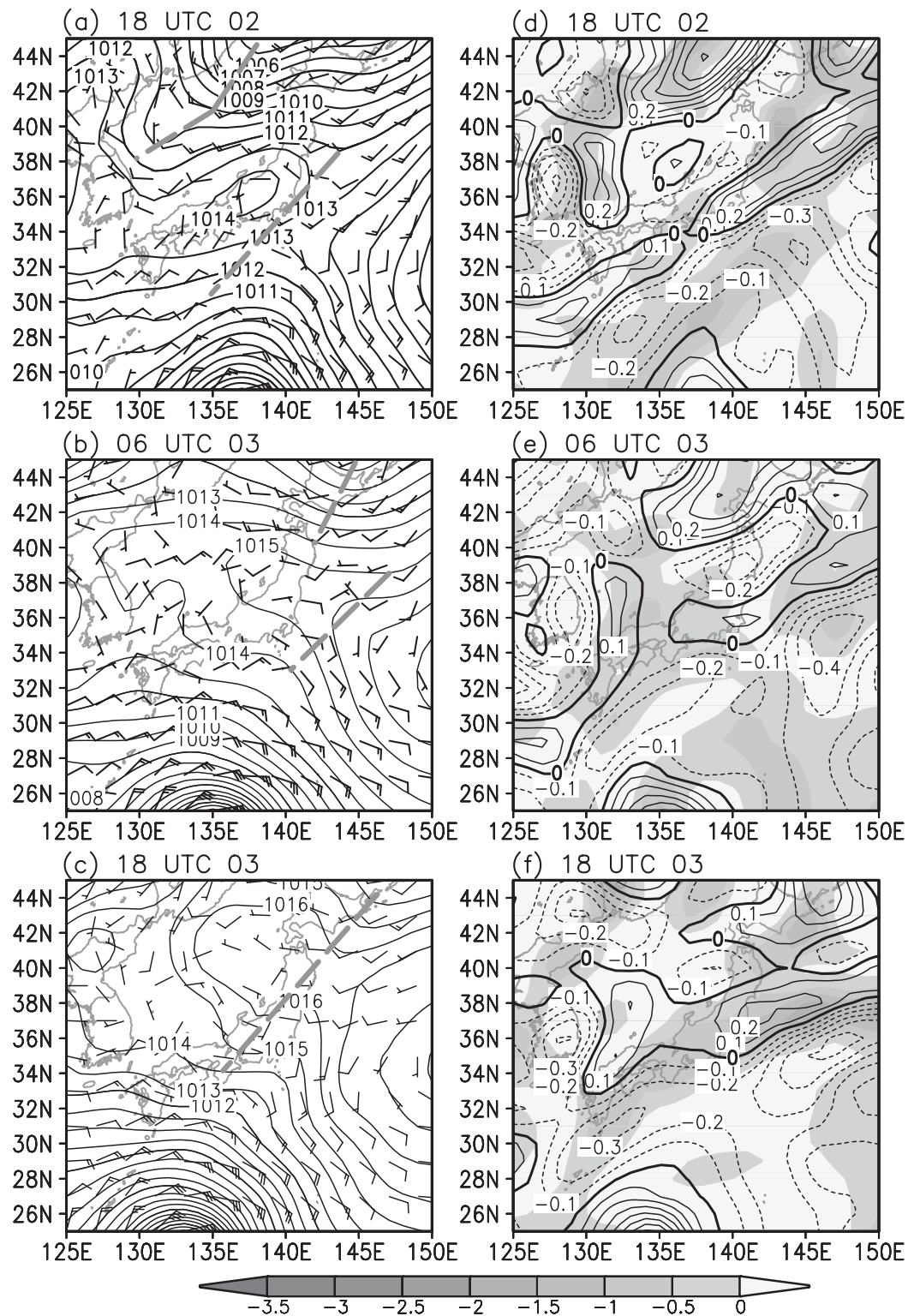


FIG. 3. (left) The 10-m wind (wind barsbs) and sea level pressure (contours interval 1 hPa) fields and (right) the horizontal divergence (shading in 10^{-5} s^{-1}) and relative vertical vorticity (contour interval $0.1 \times 10^{-4} \text{ s}^{-1}$) at (a),(d) 1800 UTC 2 Sep, (b),(e) 0600 UTC 3 Sep, and (c),(f) 1800 UTC 3 Sep 2004 from the FNL analysis. One flag represents 50 kt and one full barb represents 10 kt. Thick dashed line segments in (a)–(c) show either a short-wave trough in the midlatitude westerlies or a cyclonic shear line in the surface wind fields.

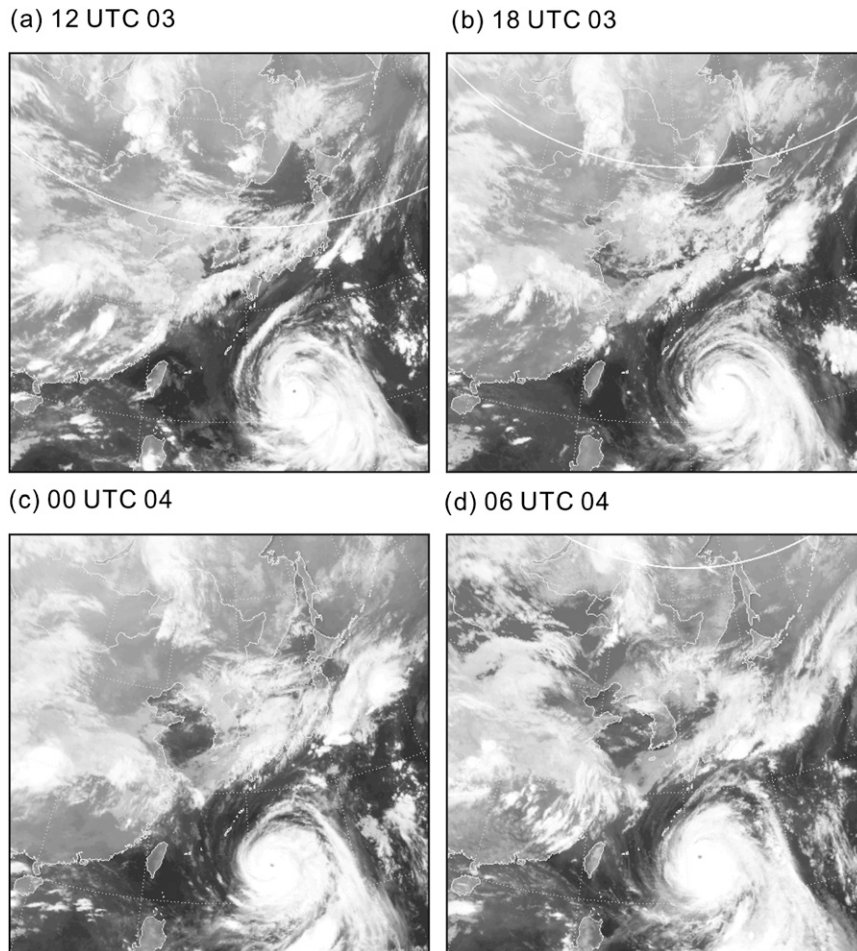


FIG. 4. Satellite images over East Asia and western North Pacific (obtained from the Korean Meteorological Administration), showing the evolution of Typhoon Songda (2004) and the precipitation system over southern central Japan and its adjacent seas with the time given at the top of each panel.

experiment (CNTRL) was designed to reproduce the observed nature discussed in section 2. Typhoon Songda (2004) from the FNL analysis (Fig. 5a) was too weak compared with the best track and observations, partly because of the small number of conventional observations over the open ocean and partly because of the coarse-resolution global model used in the data assimilation for the FNL analysis. Indeed, we could not expect the FNL analysis to depict the maximum inner-core intensity of a typhoon because of its coarse resolution and the representativeness of the grid-box mean quantities. Therefore, in order to realistically represent the typhoon in the simulation, the initial model typhoon needs to be enhanced in some way to match the observed intensity and structure. Although different methods could be used to achieve this, such as bogus data assimilation (DBA; e.g., Zou and Xiao 2000; Xiao et al. 2000), we chose a simple bogussing scheme in this study (Wang

1998). Following Wang (1998), the tangential flow (V_T) of the bogus vortex is defined by

$$V_T(r, \sigma) = V_m \left(\frac{r}{r_m} \right) \exp \left[1 - \left(\frac{r}{r_m} \right) \right] \sin \left(\frac{\pi}{2} \sigma \right), \quad (1)$$

where r denotes the radial distance from the observed typhoon center, V_m (55 m s^{-1}) is the maximum azimuthal wind at the radius of r_m (60 km), and $\sigma = (p - p_t) / (p_s - p_t)$, with p being the pressure and p_s and p_t being the unperturbed pressure at the sea surface and at $p = 100 \text{ hPa}$, respectively. The geopotential height was calculated by a gradient wind balance on constant pressure surfaces and the temperature anomaly was obtained from the thermal wind balance. This axisymmetric vortex was inserted into the FNL analysis fields without any other special treatment, which seemed to work well for this case.

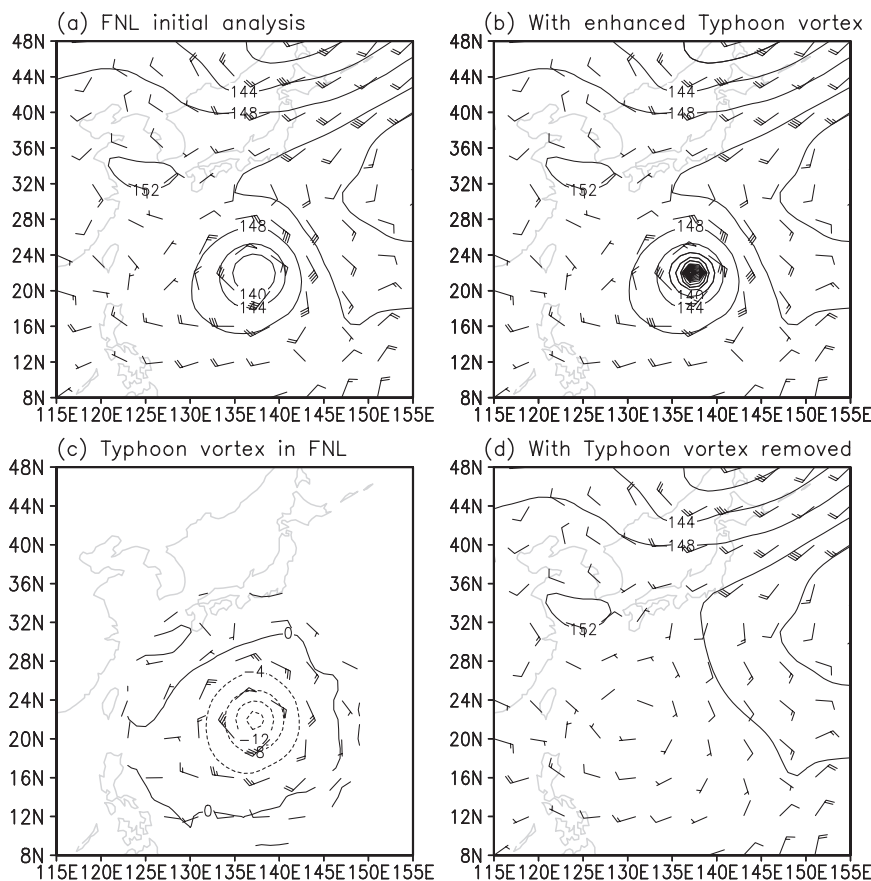


FIG. 5. Geopotential height (10 gpm contours with 40 gpm interval) and wind (barbs) fields at 850 hPa at 1800 UTC 2 Sep 2004. (a) The FNL analysis, (b) the initial conditions in the control experiment with the enhanced typhoon vortex in the FNL analysis using a bogus vortex scheme, (c) the typhoon vortex removed from the FNL analysis, and (d) the initial conditions in the No-Typhoon experiment with the typhoon vortex removed. One flag represents 50 kt and one full barb represents 10 kt.

After inserting the bogus vortex into the initial analysis, the initial model typhoon (Fig. 5b) was much stronger than that in the FNL analysis (Fig. 5a). The initial maximum wind at the 1000-hPa pressure level was increased from 20 m s^{-1} in the FNL analysis to 53 m s^{-1} (not shown), which is very close to the 56 m s^{-1} result of the Joint Typhoon Warning Center (JTWC) best track at the given time. The minimum sea level pressure was decreased from 991 hPa in the FNL analysis to 934 hPa (not shown), which is about 7 hPa higher than that given in the JTWC best track. The bogus vortex scheme enhances the inner-core structure and intensity of the initial typhoon vortex but has little effect beyond about 300 km in the FNL analysis (Fig. 6). Therefore, the initial field in the control experiment improved the representation of the typhoon vortex considerably and is suitable for this study because we mainly focus on the effects of the vortex-scale cyclonic circulation on precipitation in the remote areas.

The indirect effects of Typhoon Songda on the remote precipitation in southern central Japan in the control experiment were isolated by conducting a sensitivity experiment (No-Typhoon), in which the typhoon circulation was removed from the FNL analysis, which provided the lateral boundary conditions to the WRF model. The typhoon vortex removal algorithm used by Ross and Kurihara (1995) was adopted in this study. In our application, the successive application of a simple smoothing operator of Kurihara et al. (1990) was applied to the winds, geopotential height, temperature, and specific humidity fields of the FNL analysis centered at the observed typhoon center at a given time. Figure 5c shows the typhoon component in the FNL analysis field, and Fig. 5d shows the initial fields with the typhoon vortex removed at 850 hPa. Therefore, we can expect that the difference between the CNTRL and No-Typhoon experiments can be considered to be the effect of the typhoon on its environment.

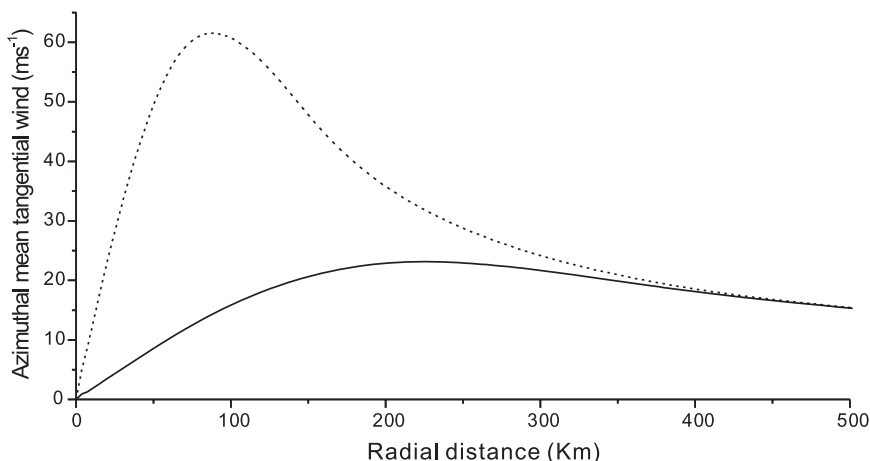


FIG. 6. Radial profiles of azimuthal mean tangential wind (m s^{-1}) at 850 hPa in the control experiment with a vortex bogus scheme (dashed) and in the No-Bogus experiment with no bogus vortex (solid) at the initial time (1800 UTC 2 Sep 2004).

Two other sensitivity experiments were also performed. The No-Bogus experiment is the same as the CNTRL experiment but without the application of the bogus scheme described above. This experiment was designed to see whether the outer circulation of the model typhoon was artificially enhanced by the bogus scheme, thus overestimating the effects of the typhoon on the remote precipitation in Japan in the CNTRL experiment. The last experiment (No-Terrain) is the same as the CNTRL experiment but with the terrain height over the main islands of Japan set to 1 m if it is higher than 1 m so that the possible effects of topography on precipitation over Japan were artificially eliminated. This experiment was intended to address whether the interaction between the outer circulation of Typhoon Songda and the orography in central Japan played any role in the heavy precipitation over Japan.

4. Verification of the control simulation

Figure 7a compares the observations and the CNTRL experiment simulated maximum 10-m height surface wind speed and minimum sea level pressure. Overall, the model simulated the intensity evolution of Typhoon Songda reasonably well, with the exception that the simulated typhoon was stronger than the observed after about 48 h of integration (Fig. 7a) due to the considerable underestimation of the weakening of Typhoon Songda. Figure 7b shows the track of Typhoon Songda from both the observations and the model simulation. Although the anticyclonic track was reproduced well by the model, the simulated track had a systematic deflection to the left of the best track. This discrepancy in the simulated track could be attributed to either the

relatively large size of the model typhoon (Wang and Holland 1996a,b), or the bias in the simulated large-scale environmental flow due to problems with the model physics, the initial data, or both. Despite the bias in the simulated track, the large-scale outer circulation of Typhoon Songda is likely similar to that observed. Therefore, the effects of Typhoon Songda on precipitation in Japan should be reasonably captured by the model in this case (see next section).

Verification of the simulated typhoon structure is challenging due to the lack of observations over the open ocean. However, the inner-core structure of the simulated storm can be compared with the Tropical Rainfall Measuring Mission (TRMM) Precipitation Radar (PR) observations. Owing to the narrow swath of the TRMM satellite, PR data are limited by sampling. What we did here was to pick up the model times that were close to the times of the PR data available to us and compare the surface rain rate from the model simulation with the PR observation.

Figure 8 shows three examples of such a comparison during 3–4 September 2004. The TRMM PR data reveal the fine structure and evolution of precipitation in the inner-core region of Typhoon Songda. In particular, Songda seemed to evolve a concentric eyewall cycle (Willoughby et al. 1982) during the given time period (left panels in Fig. 8). The model failed to reproduce the concentric eyewall cycle, however. Instead, the model simulated a relatively large eye and eyewall structure with stronger surface rain rates in the eyewall (right panels in Fig. 8). This is not surprising since the initial model typhoon did not include detailed information about the preconditioning of the concentric eyewall development and the simulation of a concentric eyewall

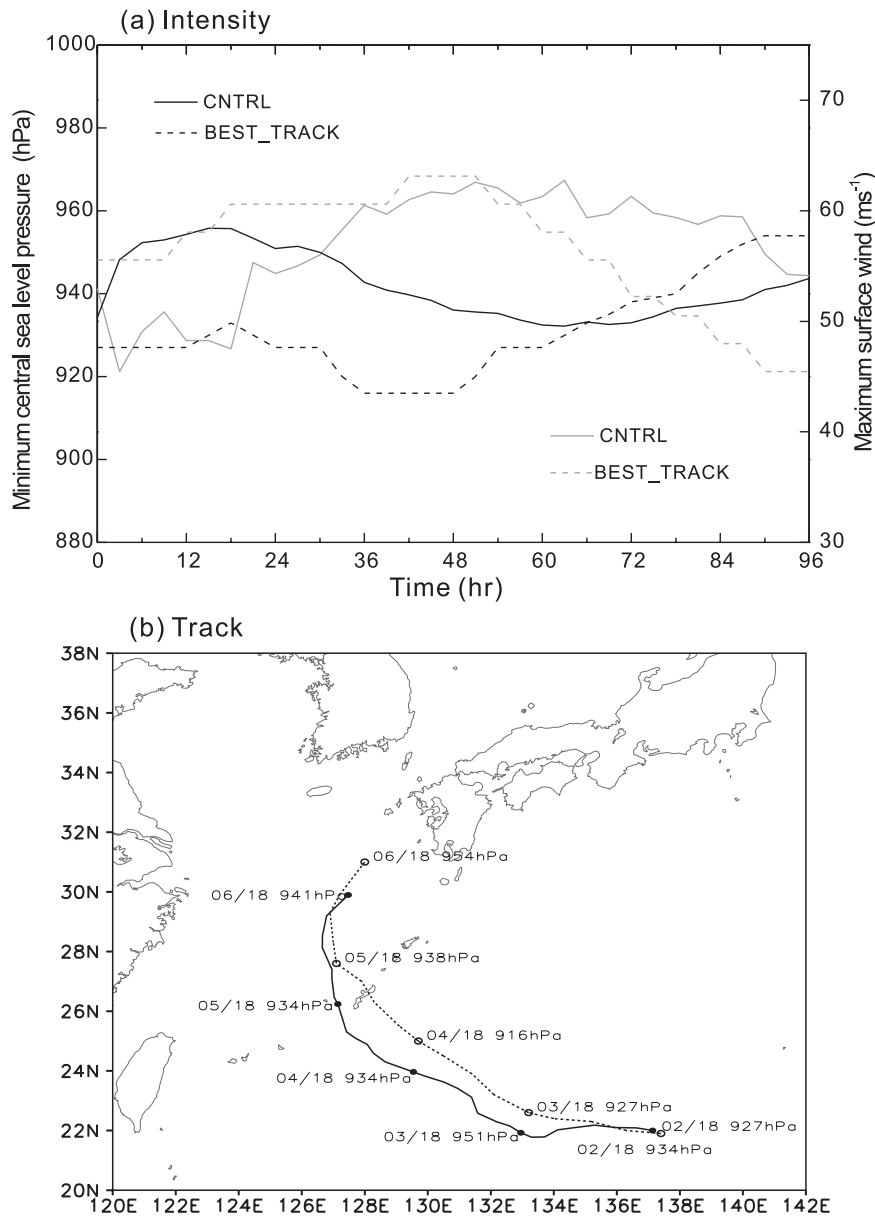


FIG. 7. (a) Evolution of the minimum central sea level pressure (hPa) and the maximum sustained 10-m wind speed (m s^{-1}) and (b) the storm track from the JTWC best track data (dashed) and the WRF model simulation in the control experiment (solid).

is still a challenging task for most numerical models (e.g., Houze et al. 2007).

Although the model did not capture the inner eyewall of Typhoon Songda, it did produce an eyewall size equivalent to the size of the outer eyewall from the TRMM PR observations. This may imply that the overall inner-core size of the model typhoon is not unrealistic compared with the real typhoon. The stronger rain rates in the simulation could be partially due to the discrepancies in the cloud microphysics scheme used in the model, in the

initial conditions, or the model resolution. Again, since the focus of this study is on the effects of the outer circulation of Typhoon Songda on remote precipitation far to the north of central Japan, the lack of concentric eyewall structure in the simulation is not expected to alter our qualitative conclusions regarding Typhoon Songda's distant effects on precipitation over Japan, which will be discussed in the next section.

The total precipitation between 1800 UTC 2 September and 0000 UTC 5 September 2004 in the control simulation

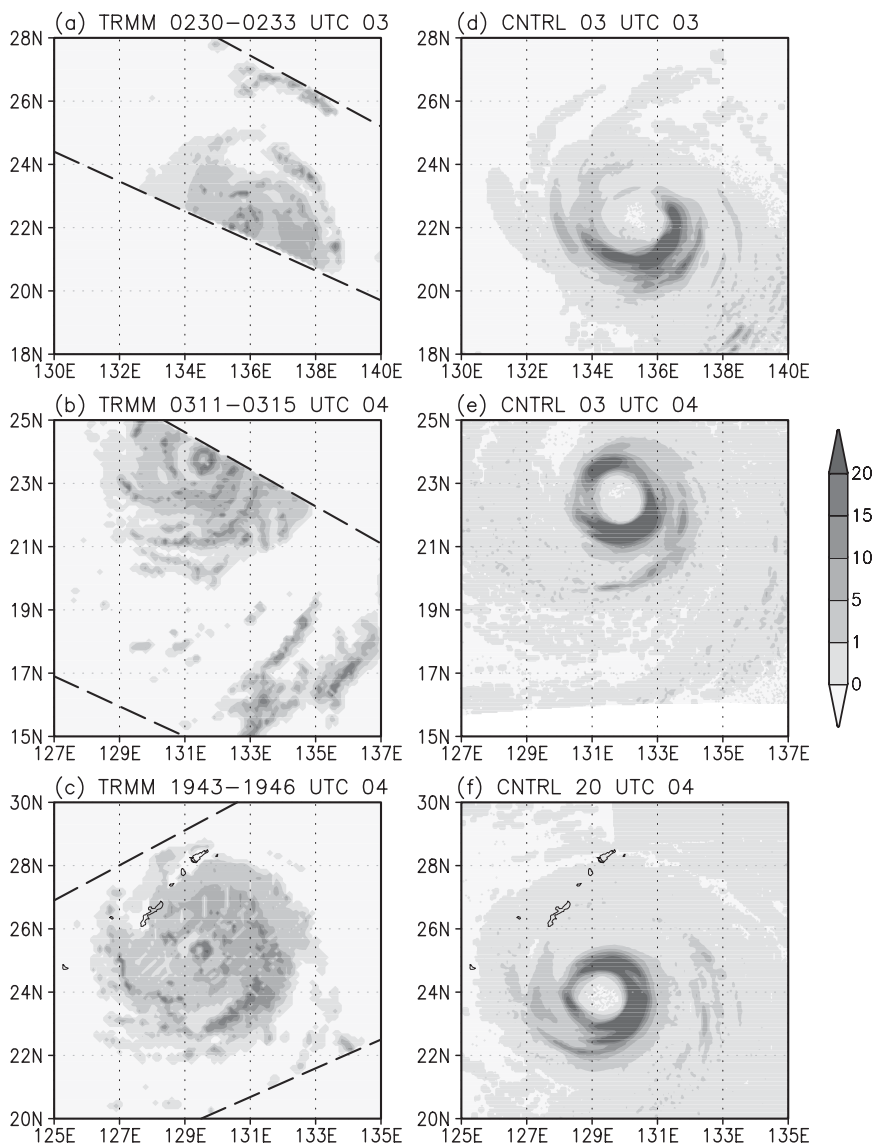


FIG. 8. Precipitation rates (mm h^{-1}) from (left) the TRMM PR data at (top) 0229:50–0233:09 UTC 3 Sep, (middle) 0311:24–0314:53 UTC 4 Sep, and (bottom) 1942:46–1946:05 UTC 4 Sep 2004 and (right) from the control experiment at (top) 0300 UTC 3 Sep, (middle) 0300 UTC 4 Sep, and (bottom) 2000 UTC 4 Sep 2004.

is shown in Fig. 9a. Compared with the total precipitation results during the same time period from the TRMM Microwave Imager (TMI) products (Fig. 1), the control experiment simulated reasonably well the observed spatial pattern of the precipitation (Fig. 9a). However, as mentioned earlier, the model overestimated the rainfall in the inner-core region along the typhoon track. The precipitation to the north over the main islands of Japan was underestimated, however. The spatial distribution of the simulated precipitation is much smoother than was observed. This may be partially due to the relatively coarse model resolution in domain 3 in this study. How-

ever, we expect that most of the discrepancies in the control simulation would not prohibit us from a qualitative assessment of the possible effects of Typhoon Songda on the remote precipitation in Japan as discussed in the next section.

5. Effects of Typhoon Songda on remote precipitation in Japan

Figure 9b shows the total precipitation from the No-Typhoon experiment during the same period as shown in Fig. 9a from the CNTRL experiment. As expected, with

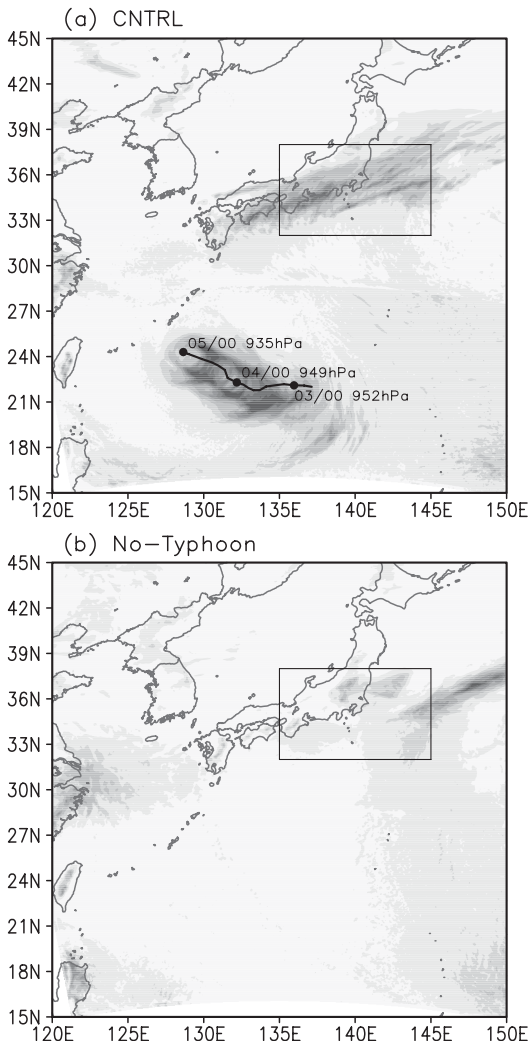


FIG. 9. Total precipitation (mm) between 1800 UTC 2 Sep and 0000 UTC 5 Sep 2004 in (a) the control experiment and (b) the No-Typhoon experiment. The typhoon track during this time period, together with the minimum central sea level pressure from the control experiment, are also shown in (a). The small box in each panel shows the area of interest, (the same as in Fig. 1) that will be used for the area means in Figs. 10 and 14.

the typhoon removed in the No-Typhoon experiment, the precipitation originally associated with Typhoon Songda over the western North Pacific almost disappeared, indicating the removal of Typhoon Songda's direct effects on precipitation along its path. In addition to the direct effects, Songda had an indirect effect on precipitation far to the north over the main island of Japan. Comparing Figs. 9a and 9b, with the typhoon removed in the No-Typhoon experiment, precipitation over the main islands of Japan and the adjacent seas was substantially reduced, suggesting that Typhoon Songda contributed positively to precipitation in Japan (rectan-

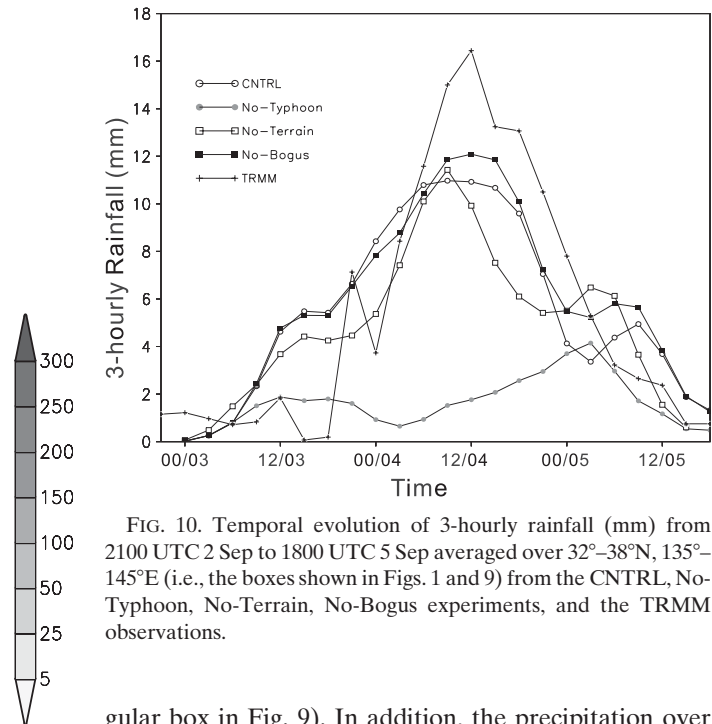


FIG. 10. Temporal evolution of 3-hourly rainfall (mm) from 2100 UTC 2 Sep to 1800 UTC 5 Sep averaged over 32°–38°N, 135°–145°E (i.e., the boxes shown in Figs. 1 and 9) from the CNTRL, No-Typhoon, No-Terrain, No-Bogus experiments, and the TRMM observations.

gular box in Fig. 9). In addition, the precipitation over the North Pacific to the east of Japan and in the lower reaches of the Yangtze River was increased slightly in the No-Typhoon experiment, implying that Typhoon Songda might play a role in suppressing precipitation in the two areas. This indirect effect could be related to the modification of the large-scale flow pattern by the typhoon outer circulation. Compared to the change in precipitation over Japan and its adjacent seas, the changes in other regions are modest. Therefore, our following analysis will focus on the effects of Typhoon Songda on remote precipitation over Japan and its adjacent seas.

Figure 10 shows the temporal evolution of the area-averaged 6-hourly rainfall in a box covering 32°–38°N, 135°–145°E (rectangular box in Fig. 9) from the TRMM TMI observations, and the CNTRL and No-Typhoon experiments. Although the CNTRL experiment underestimated the total precipitation in the given region (Fig. 9), the underestimation occurred mainly during the period from 0600 UTC 4 September to 0000 UTC 5 September 2004, namely, the period with heavy rainfall (Fig. 10). Nevertheless, the reduction in the precipitation in the region due to the removal of the typhoon is dramatic, indicating that Typhoon Songda contributed over 90% to the precipitation over Japan and its adjacent seas during 1200 UTC 3 September–0000 UTC 5 September 2005. Note that the large-scale circulation fields, in particular the short-wave trough north of 30°N in the mid- to lower troposphere in the CNTRL and No-Typhoon experiments, are similar (Figs. 11a and 11d),

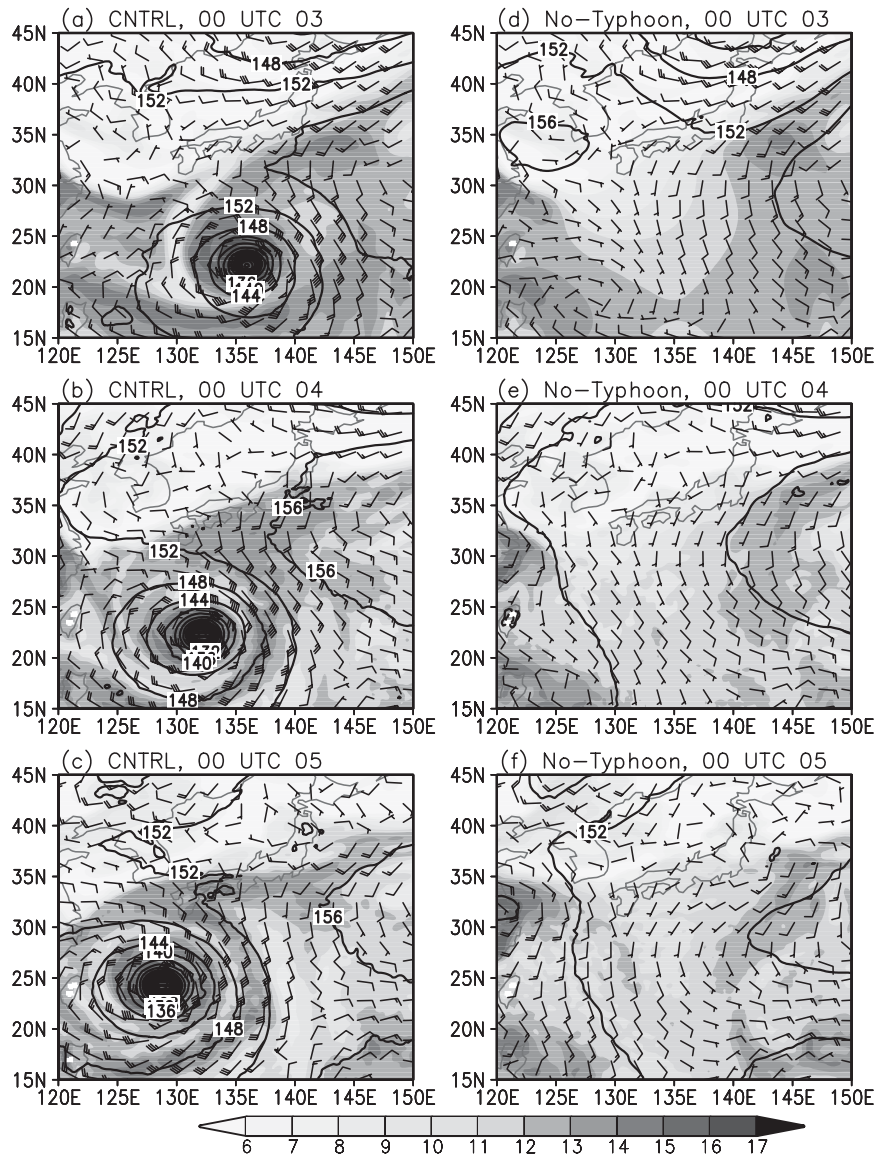


FIG. 11. Geopotential height (10 gpm contours with 40 gpm interval), specific humidity (shading, g kg^{-1}), and wind (barbs) fields at 850 hPa from (left) the control and (right) No-Typhoon experiments, respectively, at (top) 0000 UTC 3 Sep, (middle) 0000 UTC 4 Sep, and (bottom) 0000 UTC 5 Sep 2004. One flag represents 50 kt and one full barb represents 10 kt.

indicating that the preconditioned midlatitude circulation system was not substantially altered by Typhoon Songda. However, as we can see from Fig. 11, the moisture fields changed dramatically in the precipitation region over the main islands of Japan and the adjacent seas south of Japan due to the removal of Typhoon Songda. To investigate how the typhoon affected the remote precipitation in Japan, we performed a diagnostic analysis on moisture transport and two additional numerical experiments (namely, No-Bogus and No-Terrain) as discussed below.

a. Moisture transport

Typhoon Songda might significantly transport warm and moist air to the north in its northeast quadrant due to the southerly winds of its outer cyclonic circulation and the high moisture content in its circulation (left panels in Fig. 11). The southerly winds in the control experiment were also enhanced due to the increased pressure gradient between the typhoon and the subtropical high to the east (as suggested by Kawamura and Ogasawara 2006), contributing to a moisture convergence

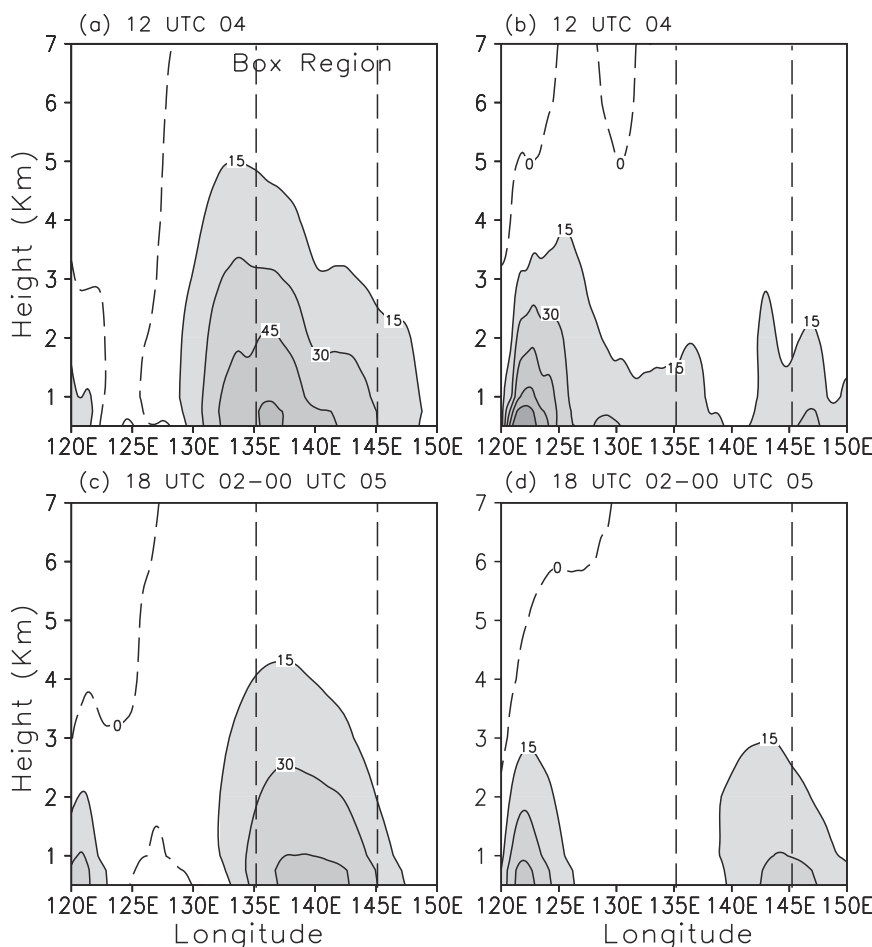


FIG. 12. Meridional moisture flux ($10^3 \text{ g m}^{-2} \text{ h}^{-1}$) across 30°N , (a),(b) at 1200 UTC 4 Sep 2004 (c),(d) averaged between 1800 UTC 2 Sep and 0000 UTC 5 Sep 2004. The control experiment is the source for (a) and (c) and the No-Typhoon experiment for (b) and (d). The contour interval is $15 \times 10^3 \text{ g m}^{-2} \text{ h}^{-1}$ and areas with values $>15 \times 10^3 \text{ g m}^{-2} \text{ h}^{-1}$ are shaded. The area of $135^\circ\text{--}145^\circ\text{E}$ (for the boxes in Figs. 1 and 9) is marked with vertical dashed lines.

zone to the north in the preconditioned precipitation region over Japan. The vertical cross section of the meridional moisture fluxes ($\rho q_v v$, where q_v is the water vapor mixing ratio and v the meridional wind speed) along 30°N for a snapshot at 1200 UTC 4 September and for an average between 1800 UTC 2 September and 0000 UTC 5 September are shown in Fig. 12. Comparing Fig. 12 (left panels) with Fig. 10, one can see that the deep layer of northward moisture transport from the CNTRL experiment contributed significantly to the precipitation in the central region of Japan. In contrast, with the typhoon removed in the No-Typhoon experiment, the southerly winds to the west of the subtropical high were much weaker than those in the CNTRL experiment, leading to a large reduction of the northward moisture transport, in particular, in the longitude band with strong precipitation in Japan.

The column-integrated moisture flux divergence is a good measure of whether the northward-transported moisture contributed to the precipitation (Banacos and Schultz 2005) in the CNTRL experiment. At a given time it can be expressed as

$$M = \int_0^{z_t} \nabla \cdot (\rho q_v \mathbf{V}) dz, \quad (2)$$

where \mathbf{V} is the horizontal wind vector, z is the height, and z_t is the height of the model top.

Figure 13 shows an example of the column-integrated moisture flux divergence at 1200 UTC 4 September, namely, at the time close to the observed maximum rainfall (Fig. 10), from the CNTRL and No-Typhoon experiments, respectively. In the CNTRL experiment, the areas with large moisture convergence are collocated

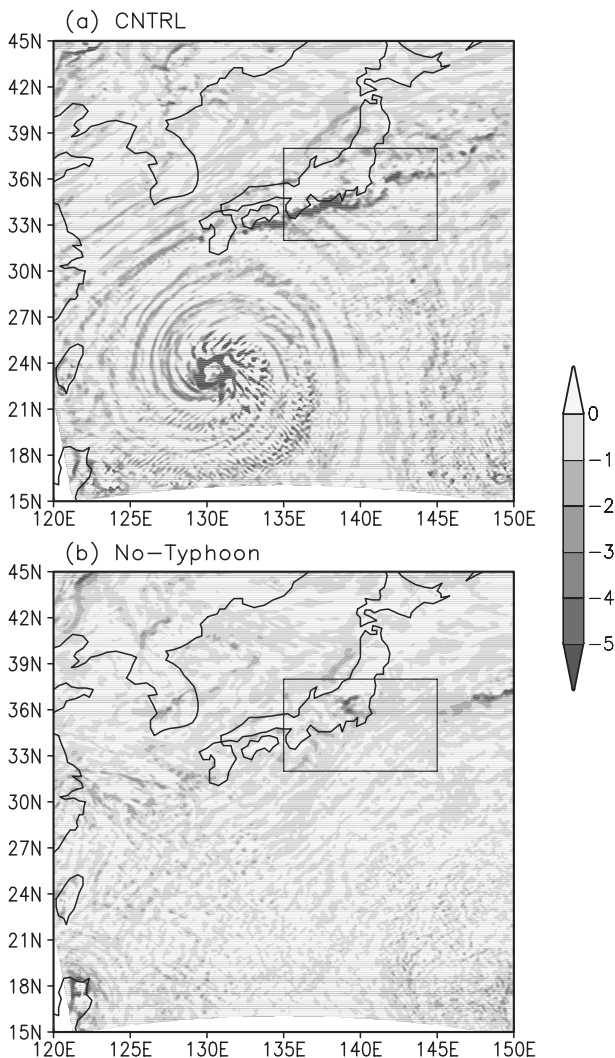


FIG. 13. Column-integrated moisture flux divergence ($10^3 \text{ g m}^{-2} \text{ h}^{-1}$) at 1200 UTC 4 Sep 2004 from the (a) control and (b) No-Typhoon experiments.

with the regions with heavy rainfall shown in Fig. 9a. The large moisture flux convergence exists in the inner-core region of the typhoon. Additionally, a northeast-southwest-elongated moisture flux convergence belt is associated with the rainfall over the main islands of Japan. With the typhoon vortex removed in the No-Typhoon experiment, the moisture flux convergence associated with the typhoon disappeared as expected, and the moisture flux convergence belt along Japan's main islands was largely suppressed, consistent with the largely reduced precipitation in the region as shown in Fig. 9b.

Figure 14 gives the temporal evolution of the area-averaged column-integrated moisture flux divergence from 1800 UTC 2 September to 1800 UTC 5 September

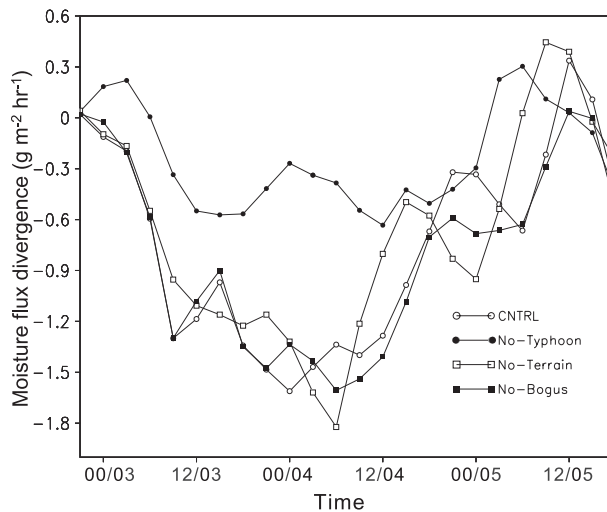


FIG. 14. The temporal evolution of the moisture flux divergence ($10^3 \text{ g m}^{-2} \text{ h}^{-1}$) averaged in the box given in Fig. 9 during 2100 UTC 2 Sep–1800 UTC 5 Sep 2004 from the control, No-Typhoon, No-Terrain, and No-Bogus experiments.

2004 from all four experiments. Comparing Figs. 14 and 10, one can find that precipitation is well correlated with, but lags, the column-integrated moisture flux convergence by about 3–6 h. Consistent with the precipitation shown in Fig. 10, the column-integrated moisture flux convergence is quite small in the No-Typhoon experiment, indicating that Typhoon Songda not only contributed to the northward moisture transport but also the moisture flux convergence in the precipitation region in Japan and the adjacent seas.

b. Effects of the bogus vortex

The indirect effects of Typhoon Songda on remote precipitation in Japan were through its outer cyclonic circulation, which significantly enhanced the northward moisture transport and contributed to the moisture convergence in the remote precipitation region. Questions arise as to whether the effects of Typhoon Songda on remote precipitation over Japan were artificially overestimated due to the introduction of a bogus vortex used in the CNTRL experiment. To address this issue, an experiment (No-Bogus) initialized with the FNL analysis without the application of the bogus vortex scheme was conducted. Although the FNL analysis cannot resolve the inner-core structure of the typhoon, it can depict reasonably well the outer circulation of the typhoon since it includes observations from a large-scale observational network and the assimilation of satellite data.

Although the simulated storm in the No-Bogus experiment was much weaker than that in the CNTRL experiment (Figs. 9a and 15a), the precipitation over Japan and its adjacent seas in the No-Bogus experiment

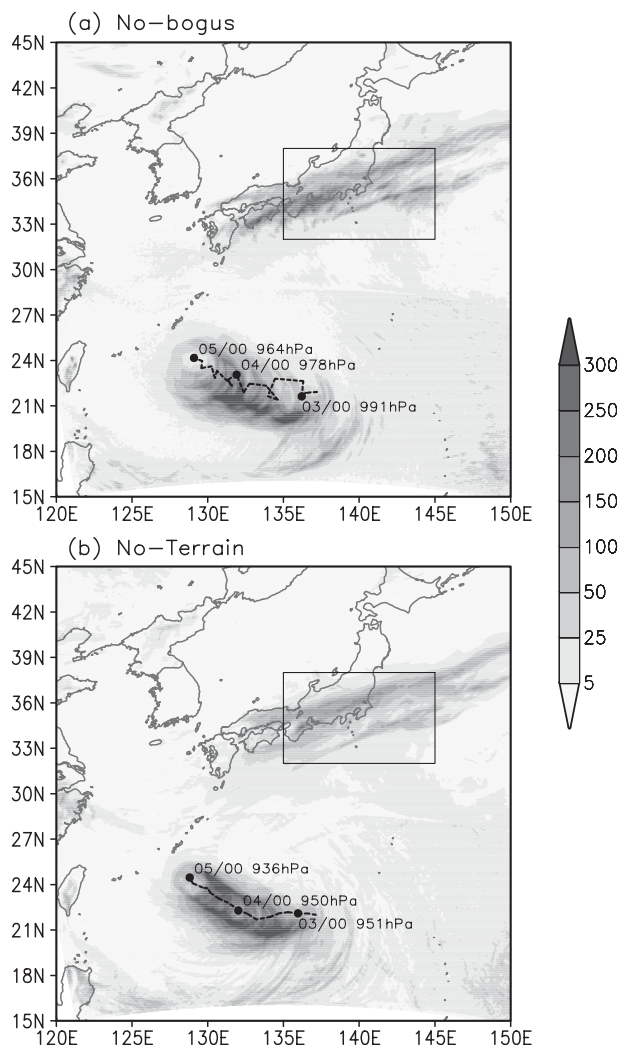


FIG. 15. Same as in Fig. 9, but for the (a) No-Bogus and (b) No-Terrain experiments.

was generally similar to that in the CNTRL experiment in both the spatial distribution in the time mean (Fig. 15a) and the temporal evolution of the area-averaged rainfall (Fig. 10). This is consistent with the similar moisture flux convergence in the No-Bogus and CNTRL experiments as shown in Fig. 14. The overall feature of the indirect effects of the model typhoon on the remote precipitation over Japan and its adjacent seas is only slightly altered even though no bogus vortex is used in the initial conditions, indicating that the initial vortex bogus mainly improved the simulation of the inner-core intensity and had little effect on the outer circulation of the storm in this case.

c. Topographic effects

Another seemingly important factor that might affect the precipitation over Japan is the orographic lifting of

warm, moist air from the southeast that could enhance precipitation along the southern slope over the mountains of central Japan. This may be the case since precipitation over Japan was to the south (windward side) of the mountainous areas in central Japan (Fig. 1). To examine this possibility, a No-Terrain experiment was conducted in which the terrain height over the main island of Japan was set to 1 m if it is higher than 1 m so that the orographic effects on precipitation over Japan would be eliminated.

The total precipitation between 1800 UTC 2 September and 0000 UTC 5 September 2004 in the No-Terrain experiment (Fig. 15b) has a spatial distribution very similar to that in the CNTRL experiment (Fig. 9a) but the precipitation amount was slightly reduced in the former. This can also be clearly seen from the temporal evolution of 6-hourly rainfall in the boxed area in Fig. 1 from the No-Terrain experiment (Fig. 10). There was no significant difference in the moisture flux divergence between the No-Terrain and CNTRL experiments (Fig. 14), indicating that the orographic lifting enhanced the precipitation over central Japan. For the case studied, the orographic forcing contributed to precipitation over Japan by about 10% and thus it is secondary to the overall precipitation process compared to the effects of Typhoon Songda.

6. Conclusions

The Advanced Research WRF model has been used to investigate the possible effects of Typhoon Songda (2004) over the western North Pacific on precipitation in a remote area to its north over central Japan and the involved physical mechanisms. In this case, when Typhoon Songda was located southeast of Okinawa, heavy rainfall occurred far to the north over southern central Japan and its adjacent seas. In a control experiment with an initial vortex enhancement algorithm, the model reasonably reproduced the major features of Typhoon Songda and the precipitation over Japan. To explicitly demonstrate the contribution of Typhoon Songda to the remote precipitation in Japan, a no-typhoon experiment was performed in which the typhoon vortex was removed from the NCEP FNL analysis fields that provided both the initial and lateral boundary conditions to the WRF-ARW model. As a result of the removal of the model typhoon, precipitation over central Japan, and the adjacent seas associated with preconditional cyclonic shear, the convergence zone was largely suppressed, indicating the dominant control of Typhoon Songda on the remote precipitation for the case studied.

The major process involved in the remote effects of Typhoon Songda is through the enhanced northward

moisture transport into the preconditioned precipitation region by its outer circulation. As a result, the presence of Typhoon Songda was critical to the observed heavy rainfall in central Japan and the adjacent seas even though the typhoon was more than 1200 km to the south over the western North Pacific. In another experiment with the terrain removed over Japan, the overall precipitation pattern was very similar to that from the control simulation except for a 10% underestimation of the precipitation, indicating that the local orographic forcing played a secondary role in the case studied.

Acknowledgments. The authors are grateful to Prof. David Schultz and Dr. Ron McTaggart-Cowan for their critical and constructive comments, which helped improve the quality of this work. This study has been supported by NSF Grants ATM-0427128 and ATM-0754029, as well as ONR Grant 000-14-06-10303. Additional support has been provided by JAMSTEC of Japan, NASA, and NOAA through their sponsorships in the International Pacific Research Center at the School of Ocean and Earth Science and Technology at the University of Hawaii.

REFERENCES

- Atallah, E., L. F. Bosart, and A. R. Ayyer, 2007: Precipitation distribution associated with landfalling tropical cyclones over the eastern United States. *Mon. Wea. Rev.*, **135**, 2185–2206.
- Banacos, P. C., and D. M. Schultz, 2005: The use of moisture flux convergence in forecasting convective initiation: Historical and operational perspectives. *Wea Forecasting*, **20**, 351–366.
- Bosart, L. F., and F. H. Carr, 1978: A case study of excessive rainfall centered around Wellsville, New York, 20–21 June 1972. *Mon. Wea. Rev.*, **106**, 348–362.
- Chen, L.-S., and Coauthors, 2006: Observations and forecast of rainfall distribution. Topic 0.3, Workshop Topic Reports of the Sixth WMO International Workshop on Tropical Cyclones (IWTC-VI), TMRP 72, WMO, 36–42.
- Chou, M.-D., and M. J. Suarez, 1994: An efficient thermal infrared radiation parameterization for use in general circulation models. NASA Tech. Memo. 104606, Vol. 3, 85 pp.
- Elsberry, R. L., 2002: Predicting hurricane landfall precipitation: Optimistic and pessimistic views from the symposium on precipitation extremes. *Bull. Amer. Meteor. Soc.*, **83**, 1333–1339.
- Farfán, L. M., and I. Fogel, 2007: Influence of tropical cyclones on humidity patterns over southern Baja California, Mexico. *Mon. Wea. Rev.*, **135**, 1208–1224.
- Ferrier, B. S., 1994: A double-moment multiple-phase four-class bulk ice scheme. Part I: Description. *J. Atmos. Sci.*, **51**, 249–280.
- Harr, P. A., D. Anwander, and S. C. Jones, 2008: Predictability associated with the downstream impacts of the extratropical transition of tropical cyclones: Methodology and a case study of Typhoon Nabi (2005). *Mon. Wea. Rev.*, **136**, 3205–3225.
- Hong, S.-Y., Y. Noh, and J. Dudhia, 2006: A new vertical diffusion package with an explicit treatment of entrainment processes. *Mon. Wea. Rev.*, **134**, 2318–2341.
- Houze, R. A., Jr., S. S. Chen, B. F. Smull, W.-C. Lee, and M. M. Bell, 2007: Hurricane intensity and eyewall replacement. *Science*, **315**, 1235–1239.
- Kain, J. S., and J. M. Fritsch, 1990: A one-dimensional entraining/detraining plume model and its application in convective parameterization. *J. Atmos. Sci.*, **47**, 2784–2802.
- Kawamura, R., and T. Ogasawara, 2006: On the role of typhoons in generating PJ teleconnection patterns over the western North Pacific in late summer. *Sci. Online Lett. Atmos.*, **2**, 37–40, doi:10.2151/sola.2006-010.
- Kimball, S. K., 2008: Structure and evolution of rainfall in numerically simulated landfalling hurricanes. *Mon. Wea. Rev.*, **136**, 3822–3847.
- Kunkel, K. E., R. A. Pielke Jr., and S. A. Changnon, 1999: Temporal fluctuations in weather and climate extremes that cause economic and human health impacts: A review. *Bull. Amer. Meteor. Soc.*, **80**, 1077–1098.
- Kurihara, Y., M. A. Bender, R. E. Tuleya, and R. J. Ross, 1990: Prediction experiments of Hurricane Gloria (1985) using a multiply nested movable mesh model. *Mon. Wea. Rev.*, **118**, 2185–2198.
- Li, Y., J.-Z. Wang, L.-S. Chen, and Y.-Q. Yang, 2007: Study on wavy distribution of rainfall associated with typhoon Masta (2005). *Chin. Sci. Bull.*, **52**, 972–983.
- Lonfat, M., R. Rogers, T. Marchok, and F. D. Marks Jr., 2007: A parametric model for predicting hurricane rainfall. *Mon. Wea. Rev.*, **135**, 3086–3096.
- Marchok, T., R. Rogers, and R. Tuleya, 2007: Validation schemes for tropical cyclone quantitative precipitation forecasts: Evaluation of operational models for U.S. landfalling cases. *Wea. Forecasting*, **22**, 726–746.
- Mlawer, E. J., S. J. Taubman, P. D. Brown, M. J. Iacono, and S. A. Clough, 1997: Radiative transfer for inhomogeneous atmosphere: RRTM, a validated correlated-*k* model for the long-wave. *J. Geophys. Res.*, **102** (D14), 16 663–16 682.
- Nakazawa, T., and K. Rajendran, 2007: Relationship between tropospheric circulation over the western North Pacific and tropical cyclone approach/landfall on Japan. *J. Meteor. Soc. Japan*, **85**, 101–114.
- Rogers, R., S. Chen, J. Tenerelli, and H. Willoughby, 2003: A numerical study of the impact of vertical shear on the distribution of rainfall in Hurricane Bonnie (1998). *Mon. Wea. Rev.*, **131**, 1577–1599.
- Ross, R. J., and Y. Kurihara, 1995: A numerical study on influences of Hurricane Gloria (1985) on the environment. *Mon. Wea. Rev.*, **123**, 332–346.
- Skamarock, W. C., and Coauthors, 2008: A description of the Advanced Research WRF version 3. NCAR Tech. Note NCAR/TN-475+STR, 113 pp.
- Smirnova, T. G., J. M. Brown, and S. G. Benjamin, 1997: Performance of different soil model configurations in simulating ground surface temperature and surface fluxes. *Mon. Wea. Rev.*, **125**, 1870–1884.
- , —, —, and D. Kim, 2000: Parameterization of cold-season processes in the MAPS land-surface scheme. *J. Geophys. Res.*, **105** (D3), 4077–4086.
- Takahashi, T., and T. Kawano, 1998: Numerical sensitivity study of rainband precipitation and evolution. *J. Atmos. Sci.*, **55**, 57–87.
- Wang, Y., 1998: On the bogusging of tropical cyclones in numerical models: The influence of vertical structure. *Meteor. Atmos. Phys.*, **65**, 153–170.

- , and G. J. Holland, 1996a: The beta drift of baroclinic vortices. Part I: Adiabatic vortices. *J. Atmos. Sci.*, **53**, 411–427.
- , and —, 1996b: The beta drift of baroclinic vortices. Part II: Diabatic vortices. *J. Atmos. Sci.*, **53**, 3737–3756.
- Willoughby, H. E., J. A. Clos, and M. G. Shoreibach, 1982: Concentric eyewalls, secondary wind maxima, and the evolution of the hurricane vortex. *J. Atmos. Sci.*, **39**, 395–411.
- Xiao, Q., X. Zou, and B. Wang, 2000: Initialization and simulation of a landfalling hurricane using a variational bogus data assimilation scheme. *Mon. Wea. Rev.*, **128**, 2252–2269.
- Yamada, K., and R. Kawamura, 2007: Dynamical link between typhoon activity and the PJ teleconnection pattern from early summer to autumn as revealed by the JRA-25 reanalysis. *Sci. Online Lett. Atmos.*, **3**, 65–68, doi:10.215/sola.2007-017.
- Yokoyama, C., and Y. N. Takayabu, 2008: A statistical study on rain characteristics of tropical cyclones using TRMM satellite data. *Mon. Wea. Rev.*, **136**, 3848–3862.
- Zou, X., and Q. Xiao, 2000: Studies on the initialization and simulation of a mature hurricane using a variational bogus data assimilation scheme. *J. Atmos. Sci.*, **57**, 836–860.